Egypt. J. Chem. **Vol. 65**, No. SI13B.. pp. 1253 - 1268 (2022)

Egyptian Journal of Chemistry

http://ejchem.journals.ekb.eg/

Antimicrobial and antioxidant evaluation of newly synthesized nanomaterials of potential anticorrosion properties based on Co (II), Ni (II), Cu (II) and Zn (II) nano complexes of N-(p-methyl phenyl)-N'-Benzoyl thiourea

Khalid M. Wahdan[a] Eman S. Zarie[b*], Zaghloul I Elbialy[c]Ali M. Hassan[a], Bassem H. Heakal[d]Ahmed O. Said [e]**

[a] *Chemistry Department, Faculty of Science, Al Azhar University, Nasr City ,11884, Egypt*
[b] *Department of Therapeutic Chemistry, Institute of Pharmaceutical and Drug Industries Research, National Research Centre, Dokki 12622, Giza, Egypt*
[c] *Egyptian Organization for Standardization and Quality*
[d] *Cairo Oil Refining Company, Mostorod, Kaliobia, Egypt*
[e] *Greater Cairo Water Company, Cairo, Egypt*

Abstract

Microwave and traditional methods were used to synthesis a novel derivative of the thiourea ligand N-(p-methylphenyl)-N'-Benzoyl thiourea (MBT) and its transition metal complexes of Co (II), Ni (II), Cu (II), and Zn (II). Elemental analysis, FT-IR, mass spectroscopy, ^{1}HNMR, ^{13}CNMR, and UV-Visible were used to investigate the structure of MBT ligand and their complexes. Geometry of proposed chelate complexes was studied using electronic spectra, electron spin resonance (ESR), and magnetic susceptibility. Thermal gravimetric analysis (TGA) was used to study the solidity of complexes. X- ray diffraction XRD was used to investigate the surface morphologies of solid complexes. Antimicrobial activity of MBT ligand and their complexes was investigated. Alsoproposed chelate complexes were examined in vitro by radical scavenging activity (DPPH) to evaluate their antioxidant activity. The anticorrosion activity of the ligand was studied by weight loss method.

***Keywords*:** microwave-assisted synthesis, Thiourea derivative, antibacterial and antifungal activity, DPPH radical scavenging and anticorrosion activity

1. Introduction

Paul Ehrlich defines chemotherapy that the use of drugs to affect the invading organism without affecting the host [1]. Ehrlich thought that it can be possible to make certain chemicals that kill bacteria and not harming the host tissue. Glutathione and other thiols are produced by the human defense system, which reduce sodium nitroprusside and reactive oxygen species. However, supplementation with exogenous antioxidant agents is required for neurodegenerative illnesses. As a result, the focus has shifted to the use of artificial antioxidants that prevent lipid peroxidation and shield against free radical destruction [2]. Antioxidants also play an important role as corrosive inhibitor as they can inhibit oxidation process. Organometallic compounds have wonderful interest due to the variation in their structure activity, in addition to physico-chemical properties and the hopeful uses in different areas [3]. Due to their chemical properties, metal ions play a vital part for many biological macromolecules structure and play a critical role in biological processes such as metabolism and medicinal chemistry [3-5]. Many compounds contain carbonyl and thiocarbonyl groups, which can be exploited as possible donor ligands [6,7]. Derivatives of thiourea ligands that were previously utilized to produce stable compounds. Thiourea $(NH_2)2C=S$ is a urea molecule with a Sulphur atom in place of the oxygen atom. They can bind to metals as a neutral, act as monodentate or bidentate ligand [8,9]. A proposed compound must be properly aimed for a microbiological agent or treat disease. Microbicidal, bactericidal, fungicidal, antimalarial, anti-tuberculosis, and antitumor properties have been described for ligands derived from thiourea and their complexes. [10-12]. In addition, produce a variety of complexes with various symmetries with several

*Corresponding author e-mail: * *eman.said.zarie1@gmail.com,**e-mail: alimhassanuk@yahoo.co.uk*
Received 19 June 2022; revised 29.June 2022; accepted 3July2022
DOI: 10.21608/EJCHEM.2022.145699.6346

metal ions [13-15]. Given the relevance of thiourea and its derivatives, it was worthwhile to synthesis N-substituted thiourea ligands and their complexes, as it was discovered, that complexing with transition metal elements increased this activity[16,17]. Microwave-assisted irradiation was used to create complexes and has several advantages ,including solvent free, faster reaction times, cleaner results, and lower costs [18, 19].

2. Materials and experimental methods

2.1 Chemical and measurements

Chemicals were purchased from Sigma Aldrich and were of Annular quality, while metal salts came from El Nasr Pharmaceutical Co. MW synthesis was performed within a home microwave with a power output ranged from 90- 900 W. Thin-layer chromatography (TLC) was used to determine the purity of the ligand and their complexes. The Electrothermal Melting PointBarnstead Thermolyne Mel-temp 1001D was used to measure melting points in open capillaries. Elemental analysis was performed on a CHNS Vario El III-Elementar automated analyzer in Germany. Samples were processed using (CsBr) powder for FT-IR spectra, then pressed as a disk and recorded on Shimadzu FT-IR spectrometer. The Mass GC-2010 Shimdazu instrument was used to determine mass spectra. Traditional titration with xylenol orange as an indicator in the present of hexamine at a buffer (pH = 6) was used to assess metal concentration. The electronic spectra of compounds in DMF solution were obtained utilizing an automated Shimadzu UV/Vis-NIR 3101 PC spectrophotometer in rang 200-900 nm.The chemical shifts ^{1}HNMR were measured in ppm compared with TMS as an internal standard in a 300MHz Varian-Oxford Mercury spectrum for Schiff base ligand in DMSO-d6 as solvent. The faraday method was used to determine the magnetic susceptibility of powder complexes. The X-ray diffraction study (XRD) was carried out at room temperature on an XRD (D8 Discovery-Bruker Company) at 40 KV and 40 AM (1600w) with a speed scan of 0.01 and 2θ from range of 10° to 80°. Thermal analysis measurements (TGA) were performed at Micro analytical using a Shimadzu thermal analyzer model 50. X-band EMX spectrometer (Bruker, Germany) recorded. Electron paramagnetic resonance spectra of Cu (II) complex using a conventional rectangular cavity of ER 4102 with 100 KHz frequency. Using the agar well diffusion method, the ligand and its metal complexes were tested for antibacterial activity in vitro against two species of Gram-positive, Gram-negative bacteria, and two species of fungi. Using a UV-visible spectrophotometer, they were also tested for in vitro by DPPH radical scavenging activity (UV-3101PC). The weight loss method was used to investigate the corrosion rate of carbon steel coupons with and without varying doses of the produced ligand inhibitor MBT at 30^{o}C.

2.2. Synthesis of benzoyl thiocyanate

To a solution of ammonium thiocyanate (0.1mmol, 7.6 gm)in 50 ml acetone was added, dropwise of benzoyl chloride (0.1mmol, 11.62 ml) in a three-neck flask and the mixture was refluxed with stirring for 1 hour. The formed precipitate was filtered and washed with acetone and the filtrate was used for further reaction.

2.3.Synthesis of the ligand (MBT)

p-Toluidine (0.1mmol ,10.7gm) was added dropwise to Benzoyl thiocyanate in 25 ml acetone in a three-neck flask with stirring. The solution was continuously stirred for two hours. After refluxing for 6 hours, the resulting solid was collected and washed with acetone and ethanol. The pure ligand (MBT) was achieved by recrystallizing from ethanol and drying over CaCl2 anhydrous in a desiccator [20].

2.4. Synthesis of Metal Complexes

The metal acetate of Ni (II), Co (II), Zn (II), and Cu (II) were blended in (1:1) molar ratio with free ligand. The admixtures were then microwave irradiated with drops of solvent methanol. The mainly product took only 3-5 minutes to complete, and the yields were greater. The resultant product was washed in hot methanol and ether before being dry out in a desiccators under decreased pressure over CaCl2 anhydrous. TLC utilizing silica gel was used to monitor the growth of the reaction and the purity of the products, complexes yield ranges from77-85 %. Scheme 1 shows the synthesis process for the obtained compounds.

3. Results and discussion

Proton and carbon NMR, mass spectroscopy, electronic spectra UV-vis, infrared spectra FT-IR, elemental analysis and melting point were used to characterize the structure of the produced ligand N-(p-methyl phenyl)-N'-Benzoyl thiourea (MBT). This data is corresponding with the required compounds. Table 1 lists the physical and analytical parameters of compounds.

3.1. FT- IR spectrum

The predicted frequencies of (N-H), (C=O), (C-N), and (C=S) were seen in the characteristic IR bands of

thiourea ligands. Because of the existence of [NHC(=S)] and [NHC(=O)] functional groups, the coordinative comportment of the ligand towards Ni (II) and Zn (II) ions to produce complexes is hard to establish.

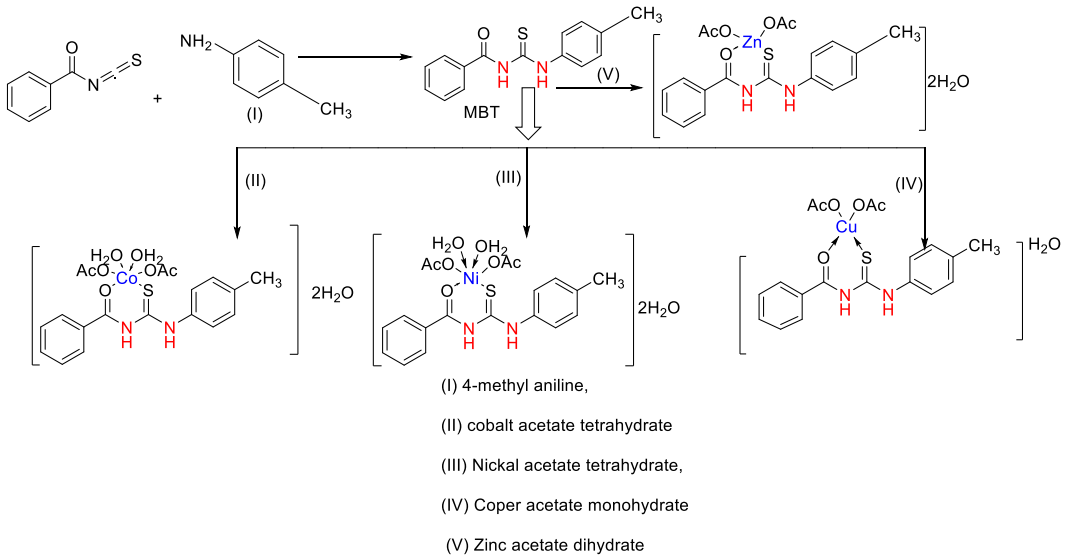

Scheme 1. MBT (N- (p-methyl phenyl)-N'-Benzoyl thiourea) and their metal Complexes Synthesis

Table 1: The synthesized compounds' analytical and physical characteristics

Compound	Molecular formula	M.Wt.	Yield %	M.p. ℃	Color	Elemental Analysis Calculated (Found)			
						%C	%H	%N	%M
MBT	$C_{15}H_{14}N_2OS$	270	77.64	160-162	yellow	66.66 (67.99)	5.185 (5.48)	10.37 (11.51)	
Co-MBT	$CoC_{19}H_{28}N_2O_9S$	519.08	78.05	343-345	Dark pink	41.47 (47.86)	5.39 (4.41)	5.39 (5.94)	11.3 (10.7)
Ni-MBT	$NiC_{19}H_{28}N_2O_9S$	519	84.56	335-337	Dark green	43.49 (48.2)	4.62 (5.39)	6.47 (5.39)	11.34 10.3)
Cu-MBT	$CuC_{19}H_{22}N_2O_6S$	469.65	78.84	345-347	Greenish	48.549 (47.26)	4.68 (4.27)	5.96 (6.06)	-
Zn-MBT	$ZnC_{19}H_{24}N_2O_7S$	489.5	81.92	305-307	Brown	46.57 (49.34)	4.9 (4.01)	5.72 (5.96)	12.59 (16.8)

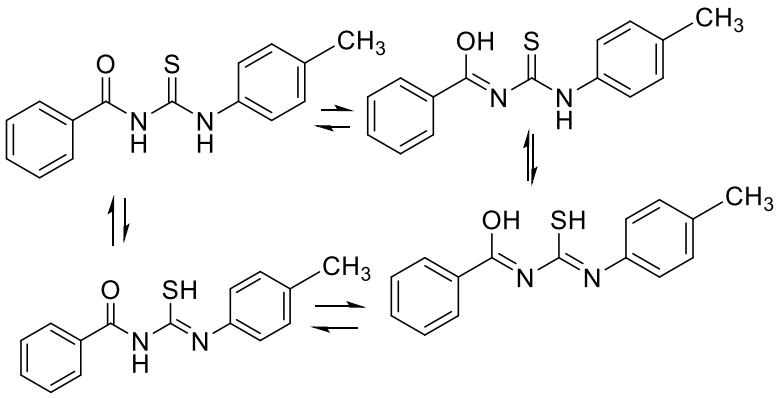

Scheme 2: Thesynthesized ligand tautomeric forms

However, the absence of (S–H) vibrations at 2500-2600 cm^{-1} as well as the presence of a peak at 3251 cm^{-1} characteristics of (N–H) that definite the deficiency of tautomeric forms (N=CSH) and (N=C-OH). Stretching vibrations of the carbonyl group as well as the thionyl group can be attributed to two acute strong bands seen at 1546 and 1355cm-1, respectively. These findings validated the ligand's ketonic thion form in the solid state [18, 19]. Furthermore, the (Ph–C) stretching frequency was discovered at 705 cm-1, whereas the band showing at 702-687 cm^{-1} was assigned to the normalvibration of phenyl ring modes. On the opposite, depending on the metal center's combination with the ligand, the distinctive peaks of (C=O, C=S) groups existing in the spectrum of MBT at 1546 and 1355cm^{-1} were discovered to be displaced, appearing from 1666 to 1689 cm^{-1} for C=O and from 1275 to 1281 cm-1 for C=S. This observation could be interpreted as proof that the oxygen and Sulphur atoms are coordinated with metal ions. Figures 1, 2, 3, 4, and 5 show the IR spectra of ligands and complexes, while table 2 lists the data.

3.2. Mass spectra

Further confirmations for the proposed structures were gained from their mass spectrum data. The mass spectrum is a robust technique that utilized to determine undetermined compounds, quantity well-known compounds and clarify the structure and chemical properties of molecules. The discovery of compounds be able to do by using small quantities. The mass spectroscopy is a method for determining the mass of an atom, molecule, or fragment. The recorded mass spectrum of MBT (Fig.6) (Scheme 3) appear several peaks indicating consecutive degradation of the free ligand. The spectrum displays the peak at m/z = 270 correspond to the molecular ion peak ($C_{15}H_{14}ON_2S$) with 38.14% abundance. The base peak 100% with m/z =77.24 refers to M+ (C_6H_6). The fragmentation models of N-(p-methyl phenyl)-N'-Benzoyl thiourea is demonstrated in Scheme 3 and Figure6. The detailed mass spectrum of MBT-Cu (Fig.7) (Scheme 4) appear several peaks demonstrating consecutive degradation of the copper complex. The spectrum showing the peak m/z = 469.67 correspond to the molecular ion peak ($CuC_{19}H_{22}O_6N_2S$) with 40.11% abundance. With m/z =351, the base peak is 100 percent. Scheme 4 and Fig.7 depict the fragmentation patterns of the Cu II complex.

3.3. ^{1}HNMR spectrum

Nuclear magnetic resonance is very important tool to establish how many different environments for hydrogen atoms exist in the molecule and with the aid of the integrator how many atoms are in each, through study of fine structure (multiplicity) of peaks, it is possible to determine which hydrogen type are closed to each other. ^{1}HNMR spectrum consist of well-separated chemically shifted resonance possessing multiple fine structure due to spin-spin interaction between the magnetically different nuclei. Also, we observed that some signal of substituted of the ring protons in benzene are chemically shifted to a low field or higher field relative to benzene (parent). ^{1}H NMR spectrum (DMSO-d6), δ, ppm: 2.23 s (3H, CH_3), 7.20–8.012 m (9H, Ar), 11.49 s (1H, NH), and 12.62 s (1H, NH).

The main single assignments in the ligand's 1HNMR spectra are provided in Fig.8, TMS internal standard was recorded in DMSO-d6 as a solvent, exhibits several groups of chemical shifts corresponding to the numerous protons. Shifts were stated in ppm. The ligand (MBT) spectra show two singlet signals of NH, one at 11.49 ppm attributed to (N8-H) and the other at 12.62 ppm assigned to (N10-H). The phenyl protons are responsible for the multiples seen between 7.20 - 8.012 ppm. At 2.2 ppm corresponding to CH_3protons.

Table 2:main FT-IR bands of complexes.

Compound	υ OH (H2O)	υ N-H	υ C-H Aromatic	υ OAc Assym. /Sym.	υ C=O	υ C=S	υPh-C	υ M-O	υ M-S
MBT	--	3480	3263	--	1546	1355	705	--	--
MBT-Co	3526	3248	3017	1435	1666	1257	687	617	501
MBT-Ni	3881	3464	3016	1412	1666	1257	687	617	501
MBT-Cu	3857	3379	3032	1458	1689	1281	702	640	501
MBT-Zn	3857	3248	3016	1450	1674	1257	694	625	509

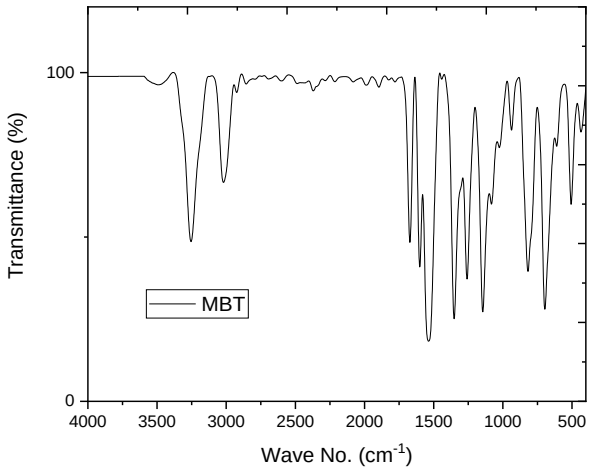

Fig.1. FT-IR spectrum of MBT ligand.

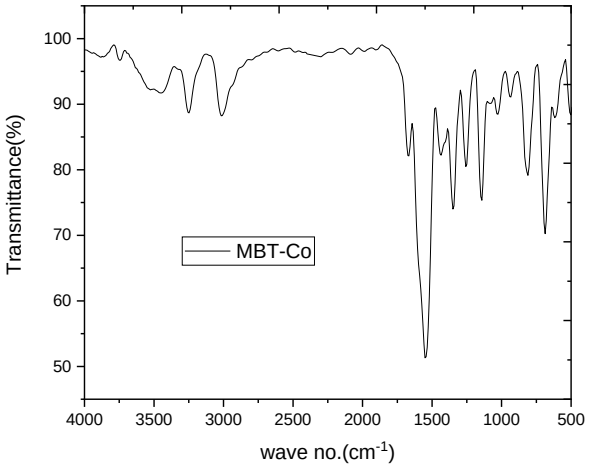

Fig.2. FT-IR spectrum of complex MBT-Co

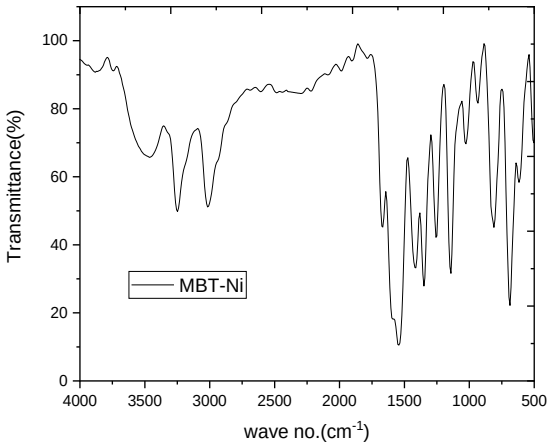

Fig.3.FT-IR spectrum of complex MBT-Ni

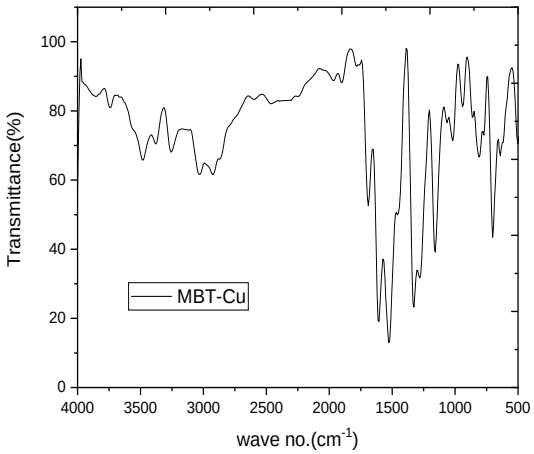

Fig.4. FT-IR spectrum of complex MBT-Cu

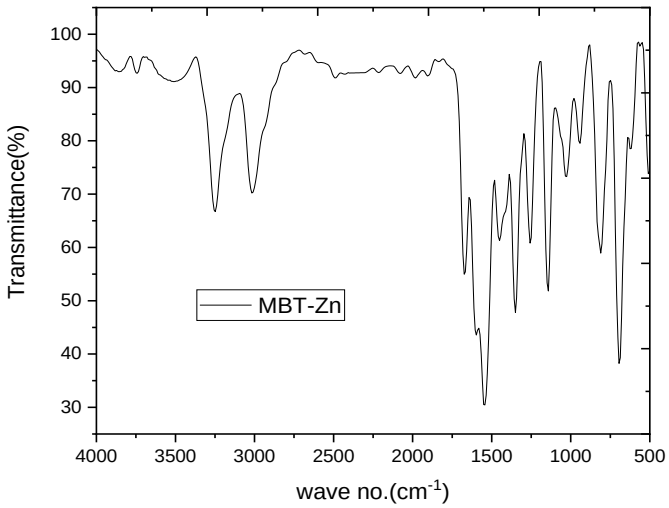

Fig.5. FT-IR spectrum of complex MBT-Zn

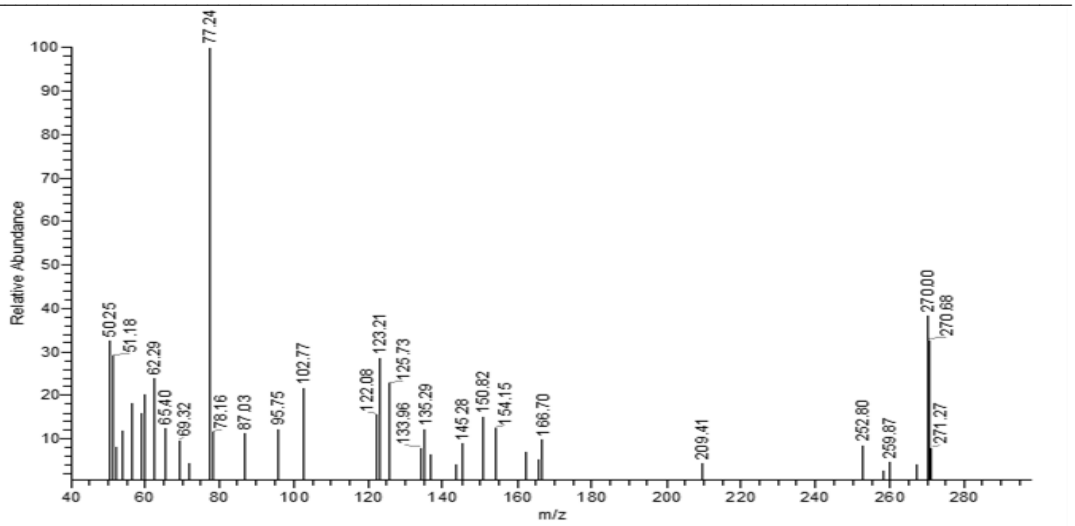

Fig. 6. MBT ligand's mass spectrum

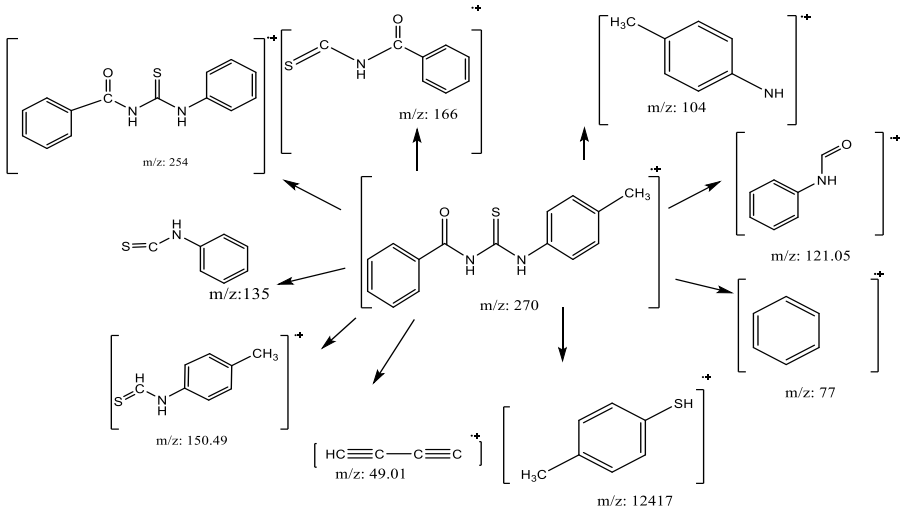

Scheme 3:Patterns of mass fragmentation of the produced ligand that have been suggested (MBT)

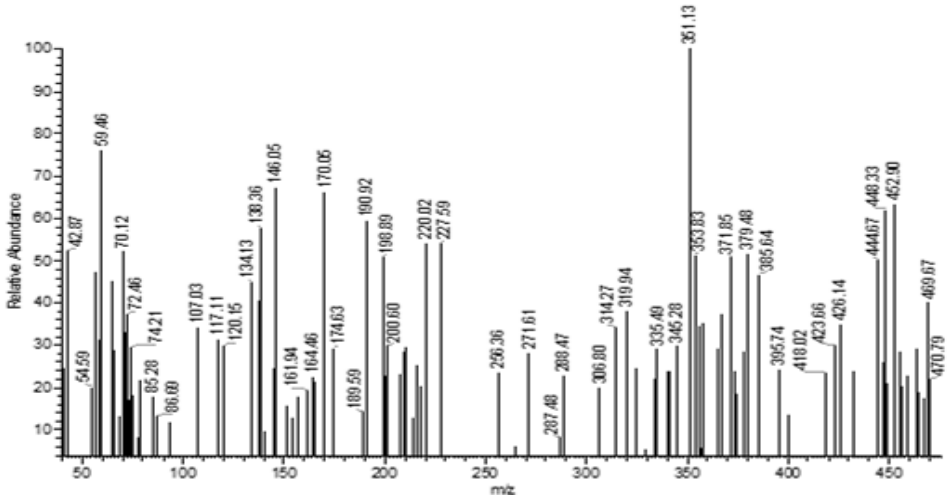

Fig. 7. Cu-MBT complex's mass spectrum.

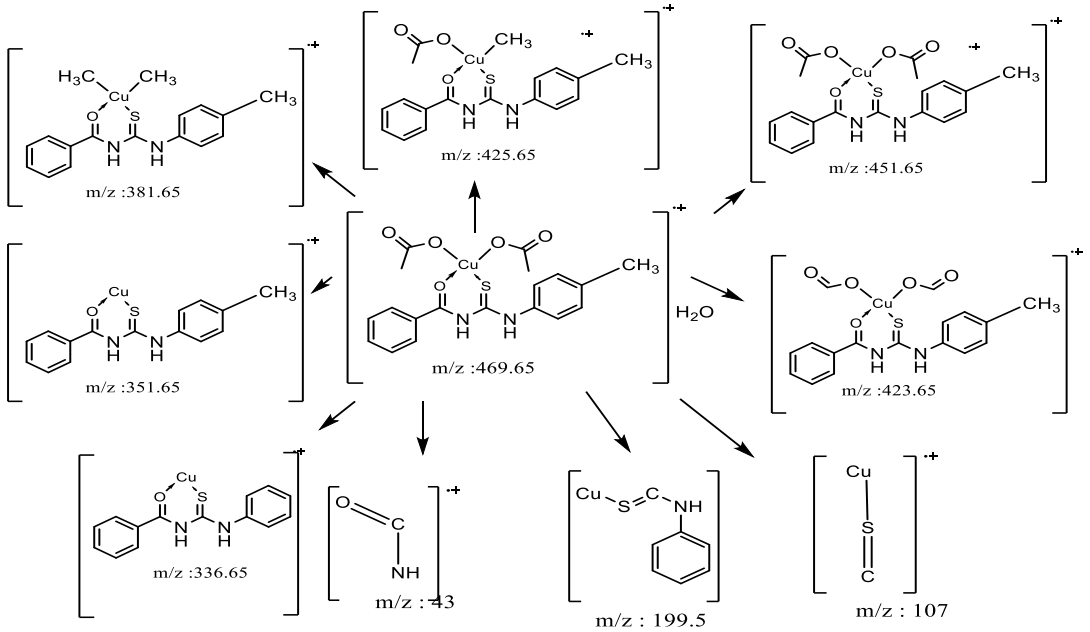

Scheme 4: Patterns of mass fragmentation of the produced ligand that have been suggested complex (Cu-MBT)

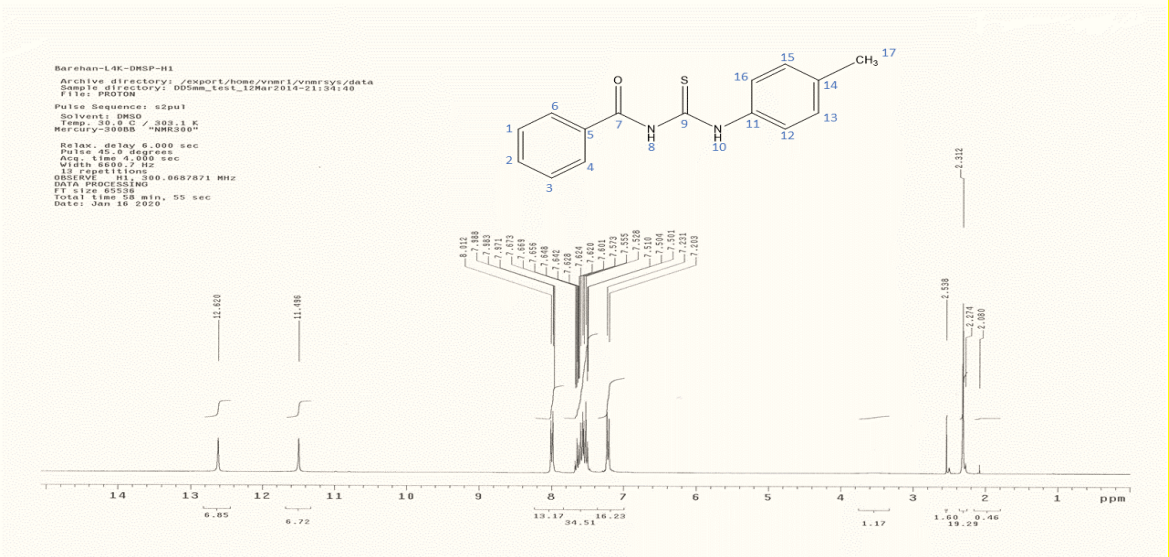

Fig.8. The MBT ligand's ^{1}H NMR spectra

3.4. ^{13}CNMR spectrum

^{13}CNMR spectra of (MBT) showed peaks at (Figure 9)178.952 ppm corresponded to (C=O), 168.313 ppm corresponded to (C=S), 135.622 ppm (C16, C13), 133.065 ppm(C5), 132.124 ppm, (C2), 129.271ppm (C15, C17) and at 129.089 ppm(C1,C3), 128.390 pm (C4 and C6) and at 20.620 ppm for C of methyl group.

3.5. Electronic spectraUV-Vis. and magnetic properties of the synthesized compounds

Electronic spectrum measurements can be used to identify the stereochemistry of metal ions in complexes. with range between 200-800 nm related to UV and visible wavelength, UV-vis spectra of the ligand and their complexes in solid state revealed numerous bands, table

3.5.1. UV-Vis. spectrum of MB For MBT ligand, absorption bands were performed at 258, 277 and 325 nm. The band at 258 nm corresponded to □–□* transitions created from aromatic ring, and bands at 277, 325 corresponded to n-□* transitions made from (C=N,C=S) groups.

3.5.2 UV-Vis. spectrumof MBT-Co

The spectrum of the MBT-Co exhibited bands at 425 to 650 nm corresponded to 4T1g (F) →4T1g (P) 4T1g (F) →4T2g transitions respectively. The observed magnetic moments of cobalt (II) complex are 7.8B.M are within the octahedral geometry.

3.5.3 UV-Vis. spectrum of MBT-Ni.

The spectrum of MBT-Ni. exhibited bands from 450 to 750 nm corresponded to 3A2g(F) -3T2g(F) (υ1), 3A2g(F)-3T1g(F) (υ2) and 3A2g(F) -3T1g(P) (υ3), as well as ligand to metal charge transfer LMCT indicating high-spin octahedral for Ni (II) complex [21]. The observed magnetic moments of nickel (II) complex are 4.99 B.M are within the octahedral geometry.

3.5.4 UV-Vis. spectrum of MBT-Cu.

The spectrum of the MBT-Cu exhibited bands from 425 to 750 nm corresponded to (2B2 → 2E) transitions [21]. The observed magnetic moments of copper (II) complex are 1.78B.M, collapses to tetrahedral geometry.

3.5.5 UV-Vis. spectrum of MBT-Zn.

The spectrum of the MBT-Zn exhibited bands from 560 to 720 (nm) which can be corresponded to MLCT in a low spin tetrahedral geometry of Zn (II) complex assured by the diamagnetic properties of complex.

Table 3 lists the assignments of the observed electronic transitions, as well as the geometry and magnetic moment values[22,23].

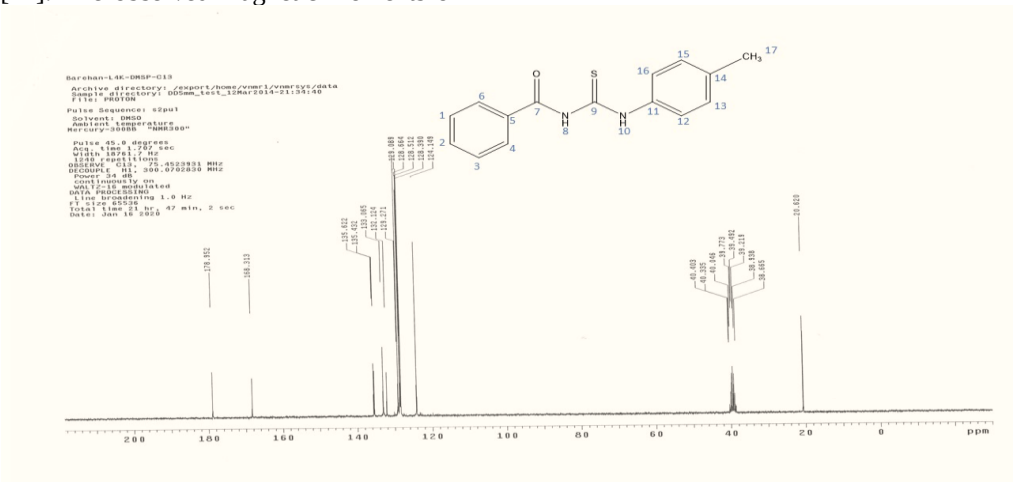

Fig.9.The MBT ligand's ^{13}CNMR spectra

Table 3: Electronic spectra and magnetic measurements of the synthesized compounds

Compound	λ_{max} nm	Assignments	$\mu_{eff.}$(B.M)	Suggested Structure
MBT	325 277 258	(n-π*, C=O), (n –π*, C=S), (π –π*, aromatic ring)	--	-
MBT-Co	425-650	^4T_1g (F) →^4T_1g(P) ^4T_1g (F)→^4T_2g	5.2	Octahedral
MBT-**Ni**	450-750	^3A_2g→^3T_1g (P) ^3A_2g→^3T_2g	3.1	Octahedral
MBT-Cu	425-750	$^2B_2$ → ^2E	1.82	Tetrahedral
MBT-**Zn**	560- 720	MLCT	Di	Tetrahedral

When matched to the spectrum of the MBT ligand and its complexes, the most important characteristics of the complex spectrum are completely different. There are certain alterations in band locations in the spectra of the complexes when the ligand interacts with metal ions.This shift can be interpreted as a sign of complex development. another proof of complex formation is the development of additional bands at longer wavelengths attributed to LMCT and d-d transitions, which provides proof for the coordination of the free ligand to the metal.

3.6.ESR Spectrum

ESR spectra are used to study chemical species with unpaired electrons can be utilized to determining the amount of electromagnetic energy absorbed by a molecular system and unpaired electrons, such as free radicals, complexes with metal ion, Copper complexes' spectrum Figure 10 shows a single broad signal with hyper structure, indicating that the free acetate ligand plays a role in complex formation. MBT-Cu showed that value of $g\backslash\backslash < g^{\perp} < 2.3$, standard of complex with 2B1 (dx2-y2) orbital ground state. The average g values for MBT-Cu were derived using the equation $gav = 1/3[g\backslash\backslash + 2g^{\perp}]$ and were 2.0669 for MBT-Cu.

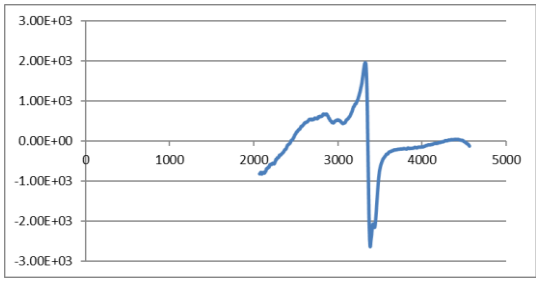

Fig.10: MBT-Cu ESR spectrum

3.7. Thermo Gravimetric Analysis (TGA):

The TGA curves show that weight loss begins about 45 °C and continues until roughly 600 °C, at which point most of the organic portion of the compounds has been lost during this rapid decomposition period, the complexes lose roughly 78 percent of their weight, resulting in the entire production of sulphides or oxides.

3.7.1. Thermal analysis of MBT ligand:

TGA curve of MBT Fig.11 refers one step of mass loss at 150-400 °C. This stage caused mass loss of 91.7% corresponded to $C_{13}H_{14}N_2OS$ leaving 2C (8.3%) as residue.

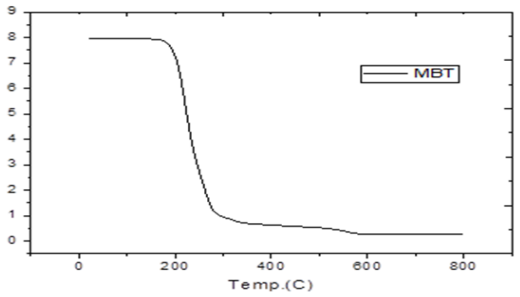

Fig.11. TGA curve of MBT

3.7.2. TGA curve of MBT-Co

The thermal decomposition process of complex MBT-Co Fig.12 indicates to double steps of mass loss at 35-800 °C. These stages include first step at temperature range 35-505 °C involved mass loss of 86.5.5 % corresponded to $4H_2O + N_2 + CS + 2AcO + 2C_6H_5 + CH_3$. The second step at the temperature rang 505-800°C losses of C_7H_5 leaving CoO (14.4 %) as residue.

3.7.3. TGA curve of MBT-Ni

The thermal decomposition process of complex MBT-Ni Fig.13 refer to three steps of mass loss at 46-585 °C. These stages include first step at temperature range 45-140°C involved mass loss of $2H_2O$. The second step at the temperature rang 140-378° C losses of $2H_2O+CO + N_2+2AcO+C_6H_5 +CH_3$. The Third step at temperature range 378-585°C involved mass loss of C_7H_5 Leaving NiS as residue 16.8%.

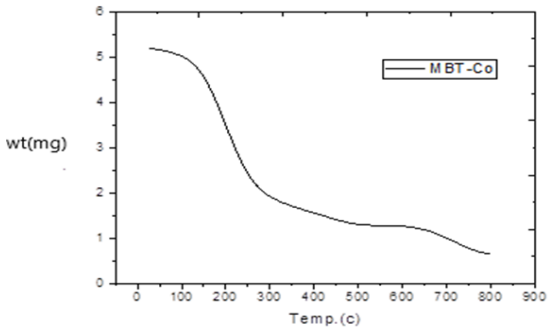

Fig.12. TGA curve of MBT-Co

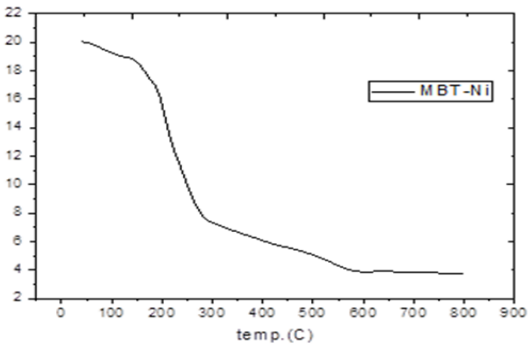

Fig.13. TGA curve of MBT-Ni

3.7.4. TGA curve of MBT-Zn

The thermal decomposition process of complex MBT-Zn Fig.14 indicates to double steps of mass losses at 45-600 °C. These stages include first step at temperature range 45-420°C involved mass loss of 86.5.5 % for $2H_2O+N_2$ +CO+2AcO+C_6H_5 +CH_3. The second step at the temperature rang 420-600°C losses of C_6H_5 leaving ZnS+C (22.34 %) as residue.

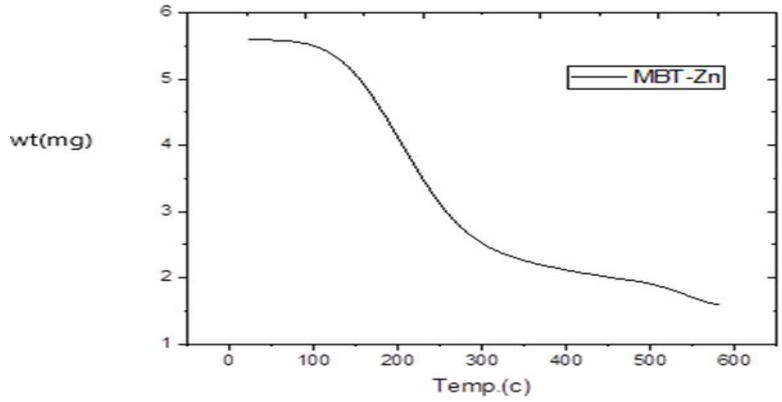

Fig.14. TGA curve of MBT-Zn

Thermal decomposition of MBT and its Complexes are expressed in scheme 5 and tabulated in table 4.

Table 4: TGA data of decomposition of MBT ligand and its Complexes.

Compund	Molecular formula	Mwt.	Steps	T_i	T_f	Calc.mass (%)	mass (%)	Assignment
MBT	$C_{15}H_{14}N_2OS$	270	1	170	400	8.8	8.3	$C_{13}H_{14}N_2OS$
MBT-Co	$CoC_{19}H_{28}N_2O_9S$	519.08	1St	35	505	31.5	25.1	$4H_2O$ N_2, CS 2AcO $2C_6H_5$ CH_3
			2nd	505	800	14.4	13.4	C_7H_5
MBT-Ni	$NiC_{19}H_{28}N_2O_9S$	519	1st	46	140	93.06	93.53	$2H_2O$
			2nd	140	378	33.3	31.4	$2H_2O$ CO N_2 2AcO C_6H_5
			3rd	378	585	16.8	16.3	CH_3 C_7H_5
MBT-Zn	$ZnC_{19}H_{24}N_2O_7S$	510	1st	45	420	36.5	36.9	$2H_2O$ N_2 ,CO 2AcO C_6H_5 CH_3
			2nd	420	600	22.34	26.84	$-C_6H_5$

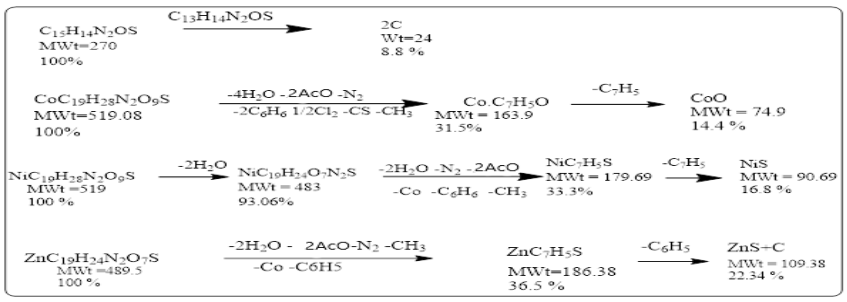

Scheme 5: MBT ligand and its complexes thermal decomposition

3.8. X- ray spectrum:

The XRD spectrum was used to get additional information about the metal complexes' structure. XRD spectrum display of the compound was scanned in 2θ values in range between 10-70° of at wavelength 1.54060Å. The data associated with the diffract gram as 2θ values for every peak, Table 5 lists relative intensity (I/I0) and inter-planar spacing (d-values). The diffract gram Fig.15 obtained for MBT-Cu indicated that this complex is crystalline in nature.

The Scherrer equation is expressed as follows**:**

$$D = \frac{K\lambda}{\beta \cos\theta}$$

From the XRD of MBT-Cu and by using Scherrer Equation crystallite size was calculated and it was found that:The average crystallite size =36.451 nm.

3.9. Scanning Electron Microscope (SEM)

The surface morphology of the complex MBT-Cu was investigated using a scanning electron microscope, which is a magnifying tool, in our research. The SEM image of the complex is given below in Figure16

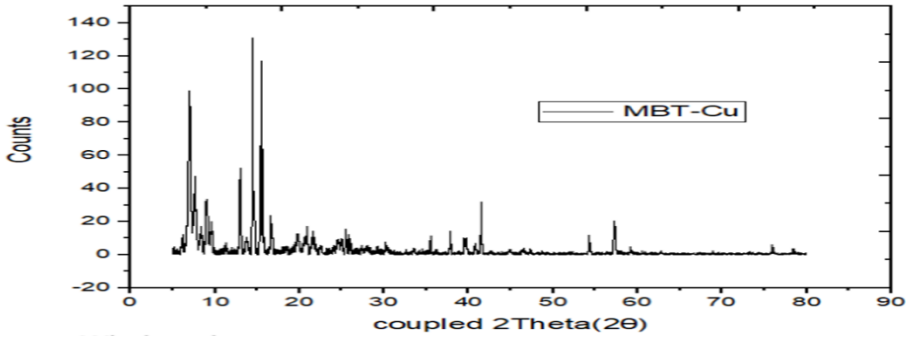

Figure 15: The X-ray diffraction of MBT-Cu.

Table 5: XRD data of MBT-Cuby using Scherrer Equation.

peak position(2theta)	FWHM		Crystallite size D(NM)	D nm(average)
6.97503	0.26785		29.71449885	**36.45101027**
14.4239	0.11079		72.27765277	
15.48677	0.39187		20.45932569	
12.99871	0.20652		38.71623177	
7.97423	2.83823		2.805820221	
20.70711	2.75037		2.936253346	
25.07722	1.72498		4.717962042	
37.84866	0.1599		52.52177976	
41.46827	0.14924		56.91802791	
57.25911	0.24194		37.40963583	
54.32154	0.10825		82.48392478	

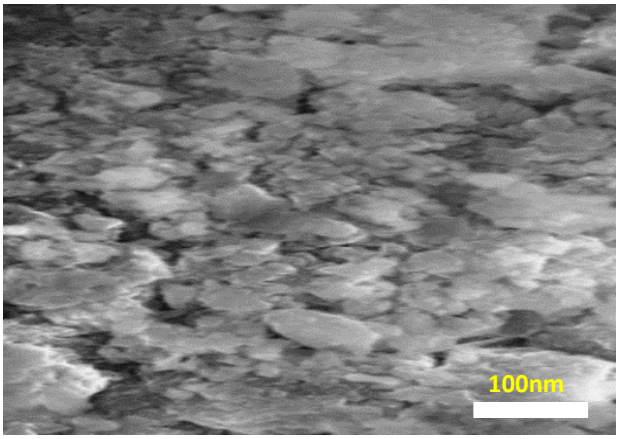

Fig. 16. The SEM image of the complex Cu-MBT

By analysis of the SEM image Table 6 it was appeared that some of the particles are in the nano scale as the average area equal to 76 nm.

4. Applications

4.1. Antimicrobial activity:

The inhibitory action of several chelates was moderately higher than corresponding free organic ligands., MBT and their copper complex were examined separately for antibacterial activity against S. aureus, streptococcus as Gram-positive bacteria, E. coli and Klebsiella.p as Gram-negative bacteria and antifungal activity against Aspergill. Antimicrobial activity against various bacteria was assessed by measuring the inhibition zone in millimeters surrounding the well and calculating the activity index data [24]. The results were compared withGentamicin as standard drug in case antimicrobial and compared with Nystatin as antifungal standard drug. The result is detailed in Table 7 and expressed in figure17.

As may be seen from the data, metal complexes reduced microorganism growth more than organic ligands (MBT) and conventional drugs. Metal complexes are extra effective bactericides and fungicides, and they may assist in ligand activation because metal ions are extra hypersensitive to bacterial cells. This performance of metal complexes is the cause of structural changes caused by coordination and the development of metal organic frameworks, and it can be described using the overtone idea and chelation theory. In general, the easy penetration of metal complexes into lipid membranes, disruption of the cell's respiration process, and preventing protein synthesis limit the organism's ability to expand further and lead to increased activity of metal complexes when compared to organic ligands.[25,26]

Table 6: Analysis of SEM image

Length	Angle	Max	Min	Mean	Area	Label
0.798	-97.125	166	130	144.667	0.088	
0.792	-90	159	144	151.556	0.088	
0.297	-90	165	91	133.5	0.039	
0.798	7.125	140.5	110	132.319	0.088	
0.714	-123.69	136.878	113	128.597	0.078	
0.68	-78.738	153.476	117.6	138.128	**0.076**	**Mean**
0.217	49.962	13.821	20.231	9.605	0.021	SD
0.297	-123.69	136.878	91	128.597	0.039	Min
0.798	7.125	166	144	151.556	0.088	Max

Table 7: Antimicrobial assay of ligand and its complex

Compound	Recorded zone diameter (mm) for each test microorganism					
	BACTRIA				FUNGI	
	Gram-positive		Gram-negative			
	Streptococcus Mutans	Staphylococcus aureus	Escherichia Coli	Klebsilla pneumonia	Asperagillus Nigar	Candida Albicans
MBT	0	10	0	20	0	10
MBT-Cu	27	26	19	25	15	18
Standard	**30**	**22**	**27**	**25**	**21**	**21**
	Gentamicin				Nystain	

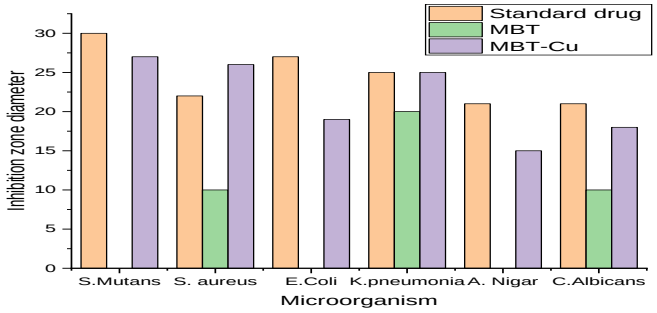

Fig.17. Antibacterial and antifungal activity of MBT and its CuII complex

4.2. Antioxidant properties:

A freshly generated methanol solution of (DPPH) radical (0.004 percent w/v) was made and stored at 1 ^{0}C in the dark. The test chemical was made into a DMSO solution. After that, the mixes were left to react in the dark for half an hour. At 515 nm, the mixed absorbance was measured spectrophotometrically [27-29]. The percentage of the DPPH radical scavenging activity of MBT and its Cu II complex was calculated, and the results was tabulated in table 8 and expressed in Figure18.

4.3. Anticorrosion Activity:

Corrosion rate of carbon steel coupons with and without different concentrations of the prepared ligand inhibitor MBT at 30 ^{o}C was studied utilizing weight loss method. The rates of corrosion were calculated from the following equation: [30]:

$$K=\Delta W /At$$

The inhibitory efficiency, w% percent, and the degree of surface covering (θ) were estimated using the equations below [30]:

$$\theta = \frac{K_0-K}{K_0}$$

$$W\ \% = \frac{K_0-K}{K_0}\times 100$$

Table 8: The percentage of the DPPH radical scavenging activity of MBT and its CuII complex

Sample concentration (µg/ml)	DPPH scavenging %(MBT)	DPPH scavenging %(MBT-Cu)
1440	54.90	83. 81
720	53.79	55.01
360	52.15	22.87
180	49.41	20.56
90	39.18	18.97
45	37.90	18.16
22.5	36.41	14.19
0	0	0

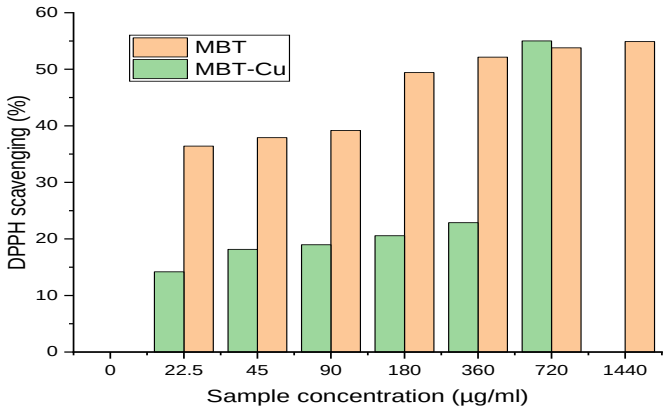

Fig.18. DPPH activity of MBT and its complex

For comparison purpose, the effect of ascorbic acid as standard antioxidant was calculated and created (IC_{50} ml) under the similar conditions table 9 and figure 19.

Table 9: The percentage of the DPPH radical scavenging activity of Ascorbic acid

Sample conc. (µg)	DPPH scavenging %
30	80.10
25	76.99
20	70.84
15	54.70
10	16.50
5	11.76
0	0

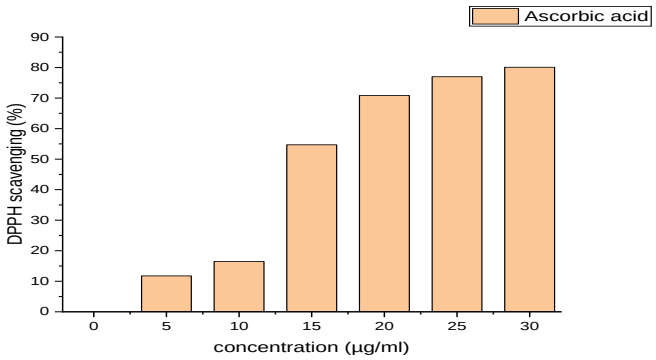

Fig.19. DPPH activityof Ascorbic acid

Table 10 shows the stated results in terms of IC_{50} value.

Table 10: IC_{50} values of Ascorbic acid and compounds under study

Compound	IC_{50} (µg/mL)
Ascorbic Acid	14.4
MBT	245
MBT-Cu	665

Table 11: weight loss in steel 1.0 M HCl without and with various ligand concentrations

Inhibitor name	Conc.(M)	k (mg cm-2 h-1)	θ	w%
Blank	0×10^{-4}	1.5916	-----	-----
MBT	0.5×10^{-4}	1.37	0.139	13.9
	0.75×10^{-4}	1.356	0.148	14.8
	2.5×10^{-4}	1.066	0.33	33
	5×10^{-4}	1.06	0.334	33.4
	7.5×10^{-4}	0.94	0.409	40.9

From Table 11 we can find that for MBT the inhibition efficiency percentage (w%) increases with increasing inhibitor concentration, this is due to an increase in mass and charge transfer to the carbon steel surface, which causes inhibitor molecules to bind to the surface and reduce metal dissolution. Also, more surface area (θ) is covered by increasing inhibitor concentration.5.

Conclusion

The compounds under investigation were successfully synthesized and analyzed utilizing elemental and spectroscopic methods. The biological activity of the ligand and the Cu II complex was then investigated and compared with reference drugs. According to the findings, the ligand and metal combination have good action and can be employed as an effective inhibitor against a variety of microbial strains. In general, this activity increased after complexation because the metal complex is more active than the ligand. Also, the antioxidant activity of the DMSO solution of the compounds under study showed slightly good antioxidant potential by DPPH when matched to standard ascorbic acid as the IC50value found to be 14.4 µg/ml for ascorbic acid, 245 µg/ml for MBT and 665 µg/ml for MBT-Cu. The complex shows lower activity than the synthesized ligand. Also, by studying the anticorrosion activity of the ligand it was found that the inhibition efficiency percentage is better than the blank and increased by increasing inhibitor concentration. So, it can be said that some of thiourea derivatives ligand and metal complexes can be useful for man health and economy as they can be considered an active inhibitor towards the different bacterial strains and have also some antioxidant and anticorrosion activity.

References

1 -Boyd R.F., General Microbiology. Times Mirror, Mosby College Publishing, St. Louis, Mo, (1988).

2-Kumar A., Varadaraj B.G., Singla R.K., Bulletin of Faculty of Pharmacy, Cairo University, Synthesis and evaluation of antioxidant activity of novel 3, 5-disubstituted-2-pyrazolines. 51(2): 167-173(2013).

3-Hassan, A. M., Said, A. O. Importance of the Applicability of O-Vanillin Schiff Base Complexes. Advanced Journal of Chemistry-Section A, 4(2), 87-103(2021).

4-Maher, K. A., Mohammed, S. R. Metal complexes of Schiff base derived from salicylaldehyde-A review. International Journal of Current Research and Review, 7(2), 6(2015).

5-Hassan A. M., Osman Said, A., Heakal B. H., Younis A., Abdelmoaz M. A., Abdrabou, M. M. Conventional and Microwave-Assisted Synthesis, Antimicrobial and Antitumor Studies of Tridentate Schiff Base Derived from O-vanillin and Phenyl Urea and its Complexes. Advanced Journal of Chemistry-Section A, 3(5), 621-638(2020).

6-Arslan H., Külcü N., Flörke U., Synthesis and characterization of copper (II), nickel (II) and cobalt (II) complexes with novel thiourea derivatives. Transition Metal Chemistry, 28(7),816-819(2003).

7-Mansuroglu D.S., Arslan H., Flörke U., Külcü N. Synthesis and characterizationof nickel and copper complexes with 2, 2-diphenyl-N-(alkyl (aryl) carbamothioyl) acetamide: the crystal structures of HL1 and cis-[Ni (L1)2]. Journal of Coordination Chemistry ,61 (19):3134-46(2008).

8-Shadab M., Aslam M. Synthesis and Characterization of some Transition Metal Complexes with N-Phenyl-N'-[Substituted Phenyl] Thiourea. Material Science Research India, 11(1):83-9(2014).

9-Arslan H, Flörke U., Külcü N., Emen M.F. Crystal structure and thermal behaviour of copper (II) and zinc (II) complexes with N-pyrrolidine-N′-(2-chloro-benzoyl) thiourea. Journal of Coordination Chemistry. 59(2), 223-228 (2006).

10-Karakuş S, Rollas SJIF. Synthesis and antituberculosis activity of new N-phenyl-N′-[4-(5-alkyl/arylamino-1, 3, 4-thiadiazole-2-yl) phenyl] thioureas. Il Farmaco, 57(7), 577-581(2002).

11-Solomon V., Haq W., Smilkstein M., Srivastava K., Puri S.K., Katti S.B. 4-Aminoquinoline derived antimalarials: synthesis, antiplasmodial activity and heme polymerization inhibition studies. European journal of medicinal chemistry,45(11):4990-4996(2010).

12-Holt S.L., Carlin R.L. Some Transition Metal Complexes of Substituted Thioureas. II. Nickel (II). American Chemical Society. 86(15): 3017-3024(1964).

13-Ke S-Y, Xue S-J. Synthesis and herbicidal activity of N-(o-fluorophenoxyacetyl) thioureas derivatives and related fusedheterocyclic compounds. Arkivoc,10:63-68 (2006).

14-Elhusseiny A.F., Eldissouky A., Al-Hamza A.M., Hassan H.H.A.M. Metal complexes of the nanosized ligand N-benzoyl-N′-(p-amino phenyl) thiourea: Synthesis, characterization, antimicrobial activity and the metal uptake capacity of its ligating resin. Journal of Molecular Structure,1100:530-545(2015).

15-Yeşilkaynak T., Özpınar C., Emen F.M., Ateş B, Kaya K., N-((5-chloropyridin-2-yl) carbamothioyl) furan-2-carboxamide and its Co (II), Ni (II) and Cu (II) complexes: Synthesis, characterization, DFT computations, thermal decomposition, antioxidant and antitumor activity. Journal of Molecular Structur,1129, 263-270(2017).

16-Fouda M, Abd-Elzaher M, Shakdofa M, El Saied F, Ayad M, El Tabl A.S., Synthesis and characterization of transition metal complexes of N′-[(1, 5-dimethyl-3-oxo-2-phenyl-2, 3-dihydro-1H-pyrazol-4-yl) methylene] thiophene-2-carbohydrazide. Transition Metal Chemistry,33(2),219-228 (2008).

17-Puglisi C., Levitus R., Chemistry N. Some substituted thiourea complexes of nickel (II) thiocyanate. Journal of inorganic and Nuclear Chemistry. 29(4), 1069-1077. (1967).

18- Hassan M., A., Heakal, B. H., Said, A. O., Aboulthana, W. M., Abdelmoaz, M. A. Comparative study for synthesis of novel Mn (II), Co (II), Ni (II), Cu (II), Zn (II) and Zr (IV) complexes under conventional methods and microwave irradiation and evaluation of their antimicrobial and Anticancer activity. Egyptian Journal of Chemistry, 63(7), 2533-2550(2020).

19-Hassan, A. M., et al. "Microwave synthesis and spectroscopic studies of some complex compounds as pigments and their applications in paints." 13(3), 517-525(2016).

20-Hassan A. M., Elbialy Z. I., Wahdan K. M. Synthesis, Characterization, Biological and Antitumor Activity of Co (II), Ni (II), Cu (II) and Zn (II) Complexes of N-(2-Chlorophenyl)-N′-Benzoyl Thiourea. Organic & Medicinal Chemistry International Journal, 9(3), 125-137(2020).

21-Yusof MSM, Khairul WM, Yamin B.M., Synthesis and characterisation a series of N-(3, 4-dichlorophenyl)-N′-(2, 3 and 4-methylbenzoyl) thiourea derivatives. Journal of Molecular Structure. 975(1-3), 280-284(2010).

22-Ali O.A., El-Medani S.M., Serea M.R.A., Sayed A.S.S., Spectroscopy B. Unsymmetrical Schiff base (ON) ligand on complexation with some transition metal ions: Synthesis, spectral characterization, antibacterial, fluorescence and thermal studies. Molecular and Biomolecular Spectroscopy, 136:651-660(2015).

23-Singh V., Singh S., Singh D., Singh P., Tiwari K., Mishra M., Butcher R.J. Synthesis, spectral and single crystal X-ray diffraction studies on Co

(II), Ni (II), Cu (II) and Zn (II) complexes with o-amino acetophenone benzoyl hydrazone. Polyhedron, 56:71-81(2013).

24-Kurt G., Sevgi F., Mercimek B. Synthesis, characterization, and antimicrobial activity of new benzoylthiourea ligands. Chemical Papers, 63(5):548-553(2009).

25-Chernyavskaya A, Loginova N, Polozov G, Shadyro O, Sheryakov A, Bondarenko E.V., Synthesis and antimicrobial activity of silver (I) and copper (II) complexes with 2-(4, 6-di-tert-butyl-2, 3-dihydroxyphenylsulfanyl) acetic acid. Pharmaceutical Chemistry Journal,40(8):413-415(2006).

26-Deswal Y. , Asija S., Kumar, D.Jindal D. K. , Chandan G. , Panwar, V., Saroya S., Kumar,N. Transition metal complexes of triazole-based bioactive ligands: synthesis, spectral characterization, antimicrobial, anticancer and molecular docking studies, Research on Chemical Intermediates ,vol. 48, 703–729 (2022)

27-Yeşilkaynak T., Muslu H., Özpınar C, Emen F.M., Demirdöğen RE, Külcü N. Novel thiourea derivative and its complexes: Synthesis, characterization, DFT computations ,thermal and electrochemical behavior, antioxidant and antitumor activities. Journal of Molecular Structure. 1142:185-193(2017).

28-Gunasekaran N., Bhuvanesh N.S.P., Karvembu R. Synthesis, characterization and catalytic oxidation property of copper (I) complexes containing monodentate acylthiourea ligands and triphenylphosphine. Polyhedron, 122, 39-45(2017).

29-Yen, G.C., Duh, P.D., Scavenging Effect of Methanolic Extracts of Peanut Hulls on Free-Radical and Active-Oxygen Species, JAgric Food Chem, 42, 629(1994).

30-Elemike E. E., Nwankwo, H. U., Onwudiwe, D. C., and Hosten, E. C. Synthesis, crystal structures, quantum chemical studies and corrosion inhibition potentials of 4-(((4-ethylphenyl)imino)methyl)phenol and (E)-4-((naphthalen-2-ylimino) methyl) phenol Schiff bases, Journal of Molecular Structure, 1147, 252-265(2017).